



DETERMINATION OF NATURAL FREQUENCIES OF A PLANAR SERIAL FLEXURE-HINGE MECHANISM USING A NEW PSEUDO-RIGID-BODY MODEL (PRBM) METHOD

Slaviša Šalinić¹, Aleksandar Nikolić²

¹ Faculty of Mechanical and Civil Engineering in Kraljevo,
The University of Kragujevac, Dositejeva 19, 36000 Kraljevo, Serbia
e-mail: salinic.slavisa@gmail.com, salinic.s@mfkv.kg.ac.rs

² Faculty of Mechanical and Civil Engineering in Kraljevo,
The University of Kragujevac, Dositejeva 19, 36000 Kraljevo, Serbia
e-mail: nikolic.a@mfkv.kg.ac.rs

Abstract

This paper presents an approach to the free vibration analysis of planar serial flexure-hinge compliant mechanisms basing on a pseudo-rigid-body method with 3-DOF (degrees of freedom) joints. The considered type of compliant mechanisms contains rigid links interconnected by flexure hinges. It is assumed that the flexure hinges undergo small in-plane deformations. Also, the masses of flexure hinges are ignored with respect to the masses of rigid links. Two lateral and one rotational springs with corresponding stiffnesses are placed in each joint in the pseudo-rigid-body model of the considered type of compliant mechanisms. The circular hinge type of flexure hinges is considered. Theoretical considerations are accompanied by a numerical example. In the numerical example a RRR compliant micro-motion stage is analyzed. The influence of the spring stiffnesses determined based on various flexure hinge compliance equations available in the literature on the vibration frequencies of the compliant mechanism is studied. Also, the comparison of accuracy in the determination of vibration frequencies of the compliant mechanism between the proposed pseudo-rigid-body method and the classical pseudo-rigid-body method (with one-DOF revolute joints) is given.

Key words: flexure hinge, pseudo-rigid-body method, compliant mechanism, RRR compliant micro-motion stage, frequencies

1. Introduction

In this paper the dynamic analysis of planar compliant mechanisms with flexure hinges of various shapes (circular notched, corner filleted, parabolic etc.) is considered. It is assumed that the elastic deformations of the flexure hinges are small. In the literature, for this purpose, various approaches were used. So, the finite element method was used in [1-4]. On the other hand, the compliance matrix method in combination with the Newton-Euler equations of motion was applied in [5,6]. Finally, the pseudo-rigid-body model (PRBM) method [7] was used in [8-11].

The PRBM method approach from [7] is based on the use of one degree of freedom (1-DOF) joint (revolute joint) with a corresponding rotational spring of a stiffness k_R (see Fig.1(b)). This type of the PRBM will be denoted by 1-PRBM. Moreover, in [12] it is proposed a new PRBM method denoted by 3-PRBM that uses a 3-DOF joint with two lateral springs of stiffness k_{L1} and k_{L2} as well as one rotational spring of a stiffness k_R (see Fig.1(c)). In Fig. 1, the quantities $\Delta\varphi$, $\Delta\xi$, and $\Delta\eta$ represent, respectively, one relative angular and two linear joint displacements.

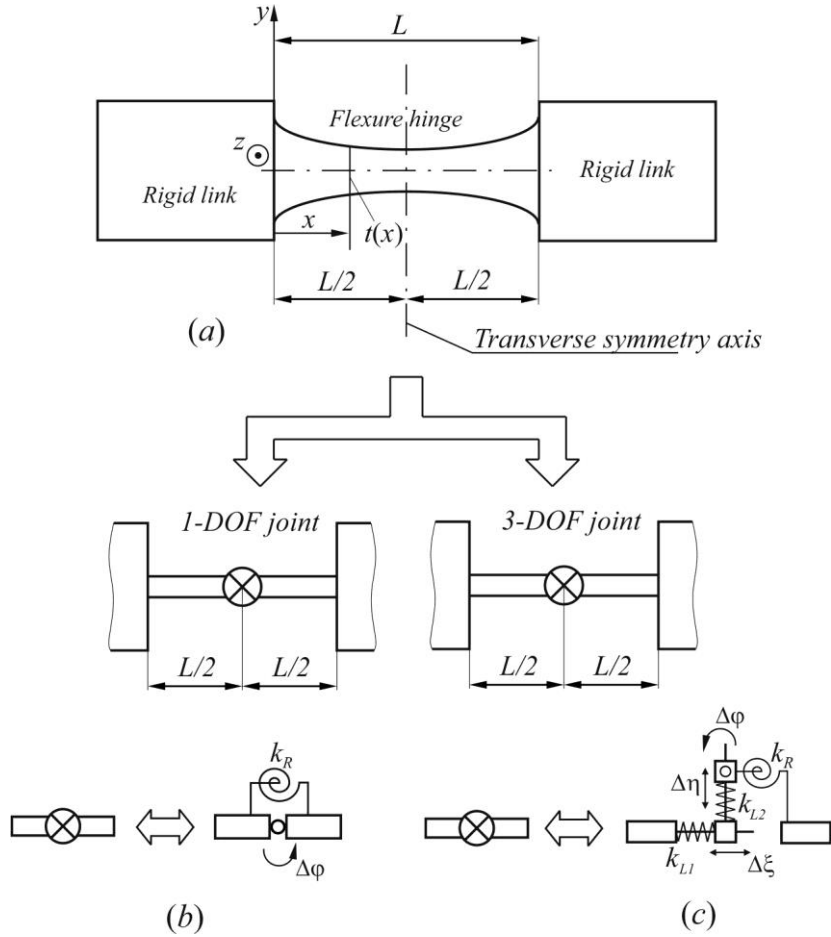


Fig. 1. Pseudo-rigid-body models of a flexure hinge with transverse symmetry axis

The stiffnesses of the springs shown in Fig. 1 are calculated as follows (see, for details, [12]):

$$k_{L1} = \frac{1}{C_a}, \quad (1)$$

$$k_{L2} = \frac{C_{b,r}}{[C_{b,t} + 2\alpha_f(1 + \mu)C_a]C_{b,r} - L^2 C_{b,r}^2 / 4}, \quad (2)$$

$$k_R = \frac{1}{C_{b,r}}, \quad (3)$$

where C_a is the axial compliance of the flexure hinge, $C_{b,t}$ is the bending translatory compliance of the flexure hinge, $C_{b,r}$ is the bending rotary compliance of the flexure hinge, μ is the Poisson's ratio, α_F is the shear correction factor ($\alpha_F = 6/5$ for the rectangular cross-section). The expression for the stiffness k_{L2} in Eq. (2) holds for the short flexure hinges with $\max(b, t(x)) < 5L$ where b is the constant out of plane width and $t(x)$ is the variable thickness of the flexure hinge (see Fig. 1). For the case of long flexure hinges with $\max(b, t(x)) \geq 5L$ one has that:

$$k_{L2} = \frac{C_{b,r}}{C_{b,t}C_{b,r} - L^2 C_{b,r}^2 / 4} \quad . \quad (4)$$

Note that the compliance coefficients C_a , $C_{b,t}$, and $C_{b,r}$ may be determined by using the Castigliano's second displacement theorem (see [2, 13]) as follows:

$$C_a = \frac{1}{Eb} \int_0^L \frac{dx}{t(x)}, \quad (5)$$

$$C_{b,t} = \frac{12}{Eb} \int_0^L \frac{x^2 dx}{t(x)^3}, \quad (6)$$

$$C_{b,r} = \frac{12}{Eb} \int_0^L \frac{dx}{t(x)^3}, \quad (7)$$

where E is the Young's modulus as well as by using the finite element analysis [19, 20] and by the integration of linear differential equations of beams [14]. The closed form symbolic expressions for the compliance coefficients defined by Eqs. (5)-(7) can be found in [2,14-16].

2. Determination of natural frequencies of a planar serial flexure-hinge mechanism

Figure 2 shows a planar serial compliant mechanism composed of flexure hinges ($\#i)(i=1, \dots, n)$ and the rigid links ($V_i)(i=0, 1, \dots, n)$. Note that the rigid link (V_0) is fixed. The flexure hinges are positioned in the horizontal plane Oxy of the inertial reference frame $Oxyz$ in which the rigid links are performing planar motion. Without loss of generality, it is assumed that adjacent rigid links are connected by the circular notched type of flexure hinges (see Fig. 3). As a rule, the gravity is ignored in the dynamic analysis of compliant mechanisms so that in the further consideration gravity is not considered. Taking this fact into account, in absence of active external forces applied to the rigid links the flexure hinges are undeformed in the equilibrium configuration of the compliant mechanism.

The 3-PRBM of the considered compliant mechanism is shown in Fig. 4 where $C_i(i=1, \dots, n)$ are the mass centers of the rigid segments, $\mathbf{r}_{C_i}(i=1, \dots, n)$ are the position vectors of the mass centers with respect to the inertial frame $Oxyz$, $\mathbf{d}_i^{(V_i)}$ and $\mathbf{d}_{i+1}^{(V_i)}$ are the position vectors of the joints J_i and J_{i+1} , respectively, relative to the mass center C_i , $O_i\xi_i\eta_i\zeta_i(i=1, \dots, n)$ are the flexure hinges local frames fixed to the rigid links

$(V_j)(j=0,1,\dots,n-1)$, respectively. In the equilibrium configuration of the compliant mechanism the axes $\xi_i(i=1,\dots,n)$ make the angles $\alpha_i(i=1,\dots,n)$ with the axis x (see Fig. 4). Note that the axes $\xi_i(i=1,\dots,n)$ coincide with the axial symmetry axes of the undeformed hinges $\#i(i=1,\dots,n)$, respectively.

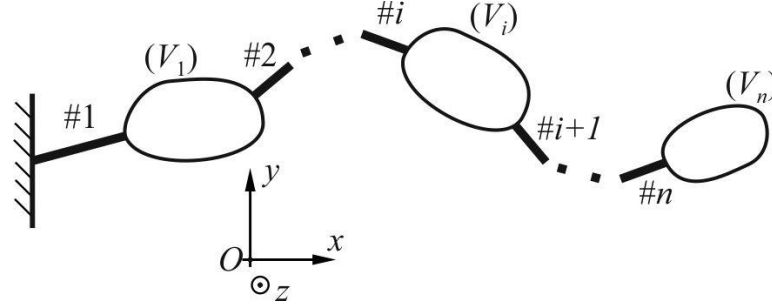


Fig. 2. A planar serial mechanism composed of rigid links and flexure hinges

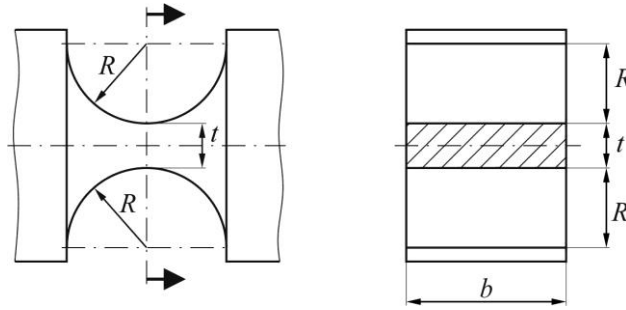


Fig. 3. A circular notched flexure hinge

Denoting by u_{ix} (displacement of the mass center C_i in the direction of x -axis), u_{iy} (displacement of the mass center C_i in the direction of y -axis), and θ_i (angular displacement of the rigid segment (V_i) in the plane Oxy) small displacements by which the displacement of the rigid segment (V_i) is described with respect to the equilibrium configuration of the compliant mechanism, the relative translatory displacements in the joints $J_i(i=1,\dots,n)$ can be written as follows (for details see [12]):

$$\mathbf{u}_{J_1} = \mathbf{A}_1 \left([u_{1x} \ u_{1y} \ 0]^T + \tilde{\Theta}_1 \mathbf{d}_1^{(V_1)} \right), \quad (8)$$

$$\mathbf{u}_{J_j} = \mathbf{A}_j \left([u_{jx} - u_{j-1x} \ u_{jy} - u_{j-1y} \ 0]^T + \tilde{\Theta}_j \mathbf{d}_j^{(V_j)} - \tilde{\Theta}_{j-1} \mathbf{d}_j^{(V_{j-1})} \right), \quad j = 2, \dots, n, \quad (9)$$

where $\mathbf{u}_{J_i} = [\Delta \xi_i \ \Delta \eta_i \ 0]^T$ ($i=1,\dots,n$) are the vectors of relative translatory displacements at the joints $J_i(i=1,\dots,n)$ expressed in the local frames $O_i \xi_i \eta_i \zeta_i$ ($i=1,\dots,n$), respectively, (see Fig.1

(c)), $\mathbf{d}_i^{(V_i)} = [d_{ix}^{(V_i)} \ d_{iy}^{(V_i)} \ 0]^T$ and $\mathbf{d}_{i+1}^{(V_i)} = [d_{i+1x}^{(V_i)} \ d_{i+1y}^{(V_i)} \ 0]^T$ are the position vectors of the joints

J_i and J_{i+1} with respect to the mass center of rigid segment (V_i) in the equilibrium configuration of the mechanism, respectively, $\tilde{\Theta}_i$ is the skew-symmetric matrix that is formed from the components of the vector $\Theta_i = [0 \ 0 \ \theta_i]^T$ in the inertial frame, and $\mathbf{A}_i \in R^{3 \times 3}$ ($i = 1, \dots, n$) are the transformation matrices of the coordinates from the inertial frame $Oxyz$ into the local hinge frames $O_i \xi_i \eta_i \zeta_i$ ($i = 1, \dots, n$), respectively, given by:

$$\mathbf{A}_i = \begin{bmatrix} \cos(\alpha_i + \theta_i) & \sin(\alpha_i + \theta_i) & 0 \\ -\sin(\alpha_i + \theta_i) & \cos(\alpha_i + \theta_i) & 0 \\ 0 & 0 & 1 \end{bmatrix} \approx \begin{bmatrix} \cos \alpha_i & \sin \alpha_i & 0 \\ -\sin \alpha_i & \cos \alpha_i & 0 \\ 0 & 0 & 1 \end{bmatrix}, \quad (10)$$

where, based on the small displacements assumption, it is taken that $\cos(\alpha_i + \theta_i) \approx \cos \alpha_i$ and $\sin(\alpha_i + \theta_i) \approx \sin \alpha_i$.

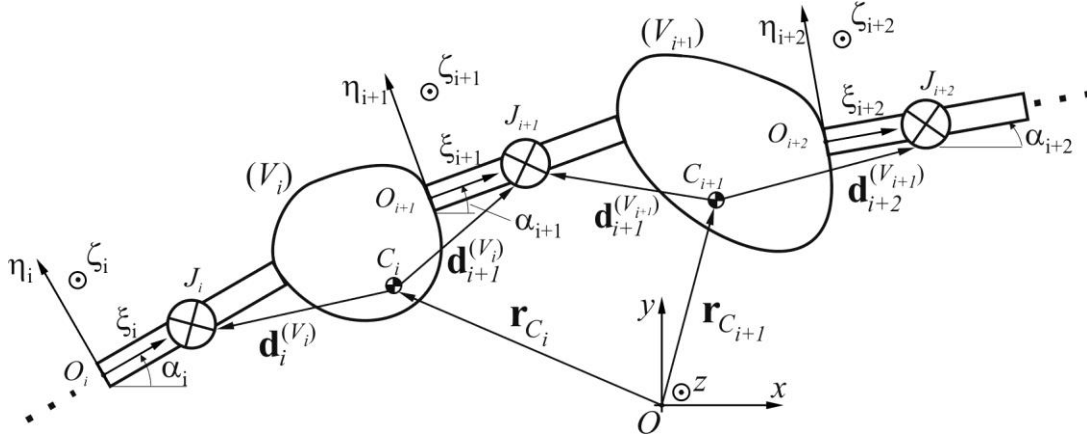


Fig. 4. The pseudo-rigid-body model of the compliant mechanism

Based on the above considerations, the potential energy of the compliant mechanism reads:

$$\Pi = \frac{1}{2} k_{R,1} \theta_1^2 + \frac{1}{2} \sum_{j=2}^n k_{R,j} (\theta_j - \theta_{j-1})^2 + \frac{1}{2} \sum_{i=1}^n k_{L1,i} \Delta \xi_i^2 + \frac{1}{2} \sum_{i=1}^n k_{L2,i} \Delta \eta_i^2, \quad (11)$$

while the kinetic energy of the mechanism is:

$$T = \frac{1}{2} \sum_{i=1}^n m_i \dot{\mathbf{r}}_{C_i}^T \dot{\mathbf{r}}_{C_i} + \frac{1}{2} \sum_{i=1}^n J_i \dot{\theta}_i^2, \quad (12)$$

where $\dot{\mathbf{r}}_{C_i} = [\dot{u}_{ix} \ \dot{u}_{iy} \ 0]^T$. Introducing the vector of generalized coordinates $\mathbf{q} = [q_1 \dots q_{3n}]^T$, where $q_i \equiv u_{ix}$ ($i = 1, \dots, n$), $q_{n+i} \equiv u_{iy}$ ($i = 1, \dots, n$), and $q_{2n+i} \equiv \theta_i$ ($i = 1, \dots, n$), the expressions for the kinetic and the potential energy can be written in the following matrix form:

$$T = \frac{1}{2} \dot{\mathbf{q}}^T \mathbf{M} \dot{\mathbf{q}}, \quad (13)$$

$$\Pi = \frac{1}{2} \mathbf{q}^T \mathbf{K} \mathbf{q}, \quad (14)$$

where $\mathbf{M} \in R^{3n \times 3n}$ and $\mathbf{K} \in R^{3n \times 3n}$ are the mass and stiffness matrices of the compliant mechanism, respectively, defined as follows:

$$M_{ik} = \frac{\partial^2 T}{\partial \dot{q}_i \partial \dot{q}_k}, \quad i, k = 1, \dots, 3n. \quad (15)$$

$$K_{ik} = \frac{\partial^2 \Pi}{\partial q_i \partial q_k}, \quad i, k = 1, \dots, 3n. \quad (16)$$

Finally, applying the Lagrange equations of the second kind [17] the differential equations describing a free vibration of the compliant mechanism read:

$$\mathbf{M} \ddot{\mathbf{q}} + \mathbf{K} \mathbf{q} = \mathbf{0}_{3n \times 1}, \quad (17)$$

where $\mathbf{0}_{3n \times 1} \in R^{3n \times 1}$ is a zero matrix. The eigenvalue problem [18] corresponding to the differential equations (17) reads:

$$(\mathbf{K} - \omega^2 \mathbf{M}) \mathbf{U} = \mathbf{0}_{3n \times 1}, \quad (18)$$

where ω is the natural angular frequency determined from the frequency equation:

$$\det(\mathbf{K} - \omega^2 \mathbf{M}) = 0, \quad (19)$$

and \mathbf{U} represents the eigenvector associated with the natural angular frequency ω . In addition, the natural frequency of the compliant mechanism is calculated as $f = \omega / (2\pi)$.

3. A numerical example

A RRR compliant micro-motion stage consisting of three rigid links, (V_1) , (V_2) , and (V_3) , and three identical circular notched flexure hinges, #1, #2, and #3, is shown in Fig. 5. Both the geometrical parameters of the rigid segments and the flexure hinges are also depicted in Fig. 5. It is taken that the compliant mechanism is made of aluminium alloy 7075 with a modulus of elasticity $E = 0.717 \times 10^{11} \text{ N/m}^2$, Poisson's ratio $\mu = 0.33$, a density $\rho = 2810 \text{ kg/m}^3$, where numerical values of the geometric parameters of the flexure hinges and the rigid links shown in Fig. 5 are (see also [19]):

$$L_1 = 15.5 \text{ mm}, \quad L_2 = 19.5 \text{ mm}, \quad L_3 = 28 \text{ mm}, \quad L_4 = 8 \text{ mm}, \quad L_5 = 10.5 \text{ mm}, \quad L_6 = 27 \text{ mm}, \\ L_7 = 31 \text{ mm}, \quad t_1 = t_2 = t_3 = 0.94 \text{ mm}, \quad R_1 = R_2 = R_3 = 1.5 \text{ mm}, \quad b = 12.7 \text{ mm}.$$

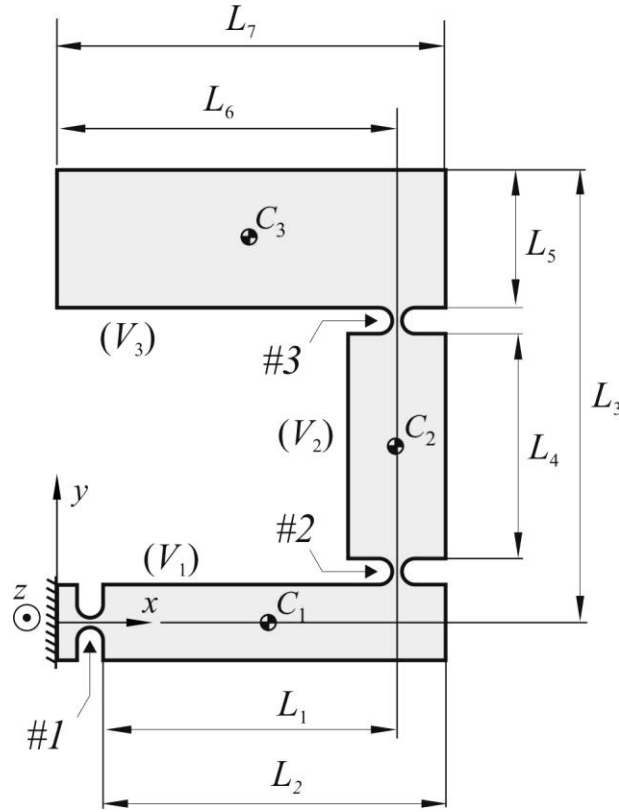


Fig. 5. The RRR compliant micro-motion stage

The eigenvalue problem defined by Eq. (18) for the considered compliant mechanism is solved for the following four cases:

- Case 1. Flexure hinge compliances calculated based on [20]:
 $C_a = 4.143 \times 10^{-9} \text{ m/N}$, $C_{b,t} = 1.561 \times 10^{-8} \text{ m/N}$, $C_{b,r} = 0.0254 \text{ rad/Nm}$
- Case 2. Flexure hinge compliances calculated based on [14]:
 $C_a = 1.534 \times 10^{-9} \text{ m/N}$, $C_{b,t} = 4.994 \times 10^{-8} \text{ m/N}$, $C_{b,r} = 0.0222 \text{ rad/Nm}$
- Case 3. Flexure hinge compliances calculated based on [2]:
 $C_a = 2.402 \times 10^{-9} \text{ m/N}$, $C_{b,t} = 5.155 \times 10^{-8} \text{ m/N}$, $C_{b,r} = 0.0204 \text{ rad/Nm}$
- Case 4. Flexure hinge compliances calculated based on [19]:
 $C_a = 2.415 \times 10^{-9} \text{ m/N}$, $C_{b,t} = 7.190 \times 10^{-8} \text{ m/N}$, $C_{b,r} = 0.0254 \text{ rad/Nm}$

In the case of the quasi-static response analysis of the RRR compliant micro-motion stage, in [19] it is shown that Case 4 gives the most accurate results when compared to the results obtained by the finite element method. So, in our paper, the vibration frequencies of the mechanism obtained for Case 4 are taken as the reference values for the calculations of percentage frequency errors for the remaining three cases. The percentage frequency errors are calculated as:

$$\frac{|f(\text{Case } i) - f(\text{Case } 4)|}{f(\text{Case } 4)} \times 100\%, \quad i = 1, 2, 3. \quad (20)$$

The first three frequencies of the RRR compliant micro-motion stage along with the corresponding percentage errors are shown in Table 1. The values shown in Table 1 show the

influence of the values of compliances C_a , $C_{b,t}$, and $C_{b,r}$ obtained based on various flexure hinge compliance equations on vibration frequencies for the RRR compliant micro-motion stage.

Case	Natural frequencies f_i (Hz)		
	f_1	f_2	f_3
Case 1	262.003 (0.12%)	512.511 (0.42%)	2283.16 (3.87%)
Case 2	280.037 (7%)	546.743 (7.13%)	2381.48 (8.34%)
Case 3	292.051 (11.6%)	569.741 (11.6%)	2462.97 (12%)
Case 4	261.698	510.368	2198.18

Table 1. The lowest three natural frequencies f_i ($i = 1, 2, 3$) for a RRR compliant micro-motion stage obtained for various flexure hinges compliances values

Finally, the comparison of accuracy in determination of natural frequencies between our PRBM method and the PRBM method based on one-DOF revolute joints for different methods of calculation of the values of compliances C_a , $C_{b,t}$, and $C_{b,r}$ is shown in Table 2.

Case	Method	Natural frequencies f_i (Hz)		
		f_1	f_2	f_3
Case 2	3-PRBM	280.037	546.743	2381.48
	1-PRBM	280.081 (0.02%)	547.109 (0.07%)	2393.06 (0.5%)
Case 3	3-PRBM	292.051	569.741	2462.97
	1-PRBM	292.176 (0.04%)	570.736 (0.17%)	2496.41 (1.4%)
Case 4	3-PRBM	261.698	510.368	2198.18
	1-PRBM	261.844 (0.06%)	511.486 (0.22%)	2237.25 (1.8%)

Table 2. The lowest three natural frequencies f_i ($i = 1, 2, 3$) for a RRR compliant micro-motion stage obtained by two different PRBM methods

The percentage frequency errors appeared in Table 2 are calculated as:

$$\frac{|f(1-PRBM) - f(3-PRBM)|}{f(3-PRBM)} \times 100\%, \quad i = 1, 2, 3. \quad (21)$$

4. Conclusions

In this paper a new pseudo-rigid-body model method based on 3-DOF joints has been proposed. The proposed method allows a relatively simple way for the determination of natural frequencies of planar serial flexure-hinge compliant mechanisms. Also, our method requires much less computational effort for the determination of natural frequencies in comparison to the finite element method [2,4] and the method based on compliance matrices and Newton-Euler equations of motion [5,6]. All relations are derived in the symbolic form which represents the benefit with solving various optimization problems of flexure based compliant mechanisms. The considerations in this paper can be easily adapted to study vibration problems of planar compliant mechanisms with tree-like and closed-loop multibody structures. In addition, the dynamic analysis of tree-like and closed-loop multibody structures using the 1-PRBM method requires the application of the differential equations of motion with the Lagrange multipliers which is not the case if the 3-PRBM method is to be used. In this sense the 3-PRBM method is more suitable than the 1-PRBM method for dynamic analysis of single-loop and multiple-loop flexure based compliant mechanisms. Also, in contrast to the 3-PRBM method, by 1-PRBM method can not be taken into account shear effects in the deformations of short flexure hinges because the stiffness k_R is the same for both short and long flexure hinges (see the expression (3)).

Acknowledgments. This research was supported by the Ministry of Education, Science and Technological Development of the Republic of Serbia (grant numbers TR35006 and ON174016). This support is gratefully acknowledged.

References

- [1] Elmustafa, A.,A., Lagally, M.,G., *Flexural-hinge guided motion nanopositioner stage for precision machining: finite element simulations*, Precision Engineering, Vol. 25, 77-81, 2001.
- [2] Lobontiu, N., *Compliant Mechanisms: Design of Flexure Hinges*, CRC Press, Boca Raton, 2003.
- [3] Wang, W., Yu, Y., *Dynamic analysis of compliant mechanisms using the finite element method*, Proceedings of the 2008 IEEE/ASME International Conference on Advanced Intelligent Mechatronics, July 2-5, 2008, Xi'an, China, 247-251, 2008.
- [4] Friedrich, R., Lammering, R., Rösner, M., *On the modeling of flexure hinge mechanisms with finite beam elements of variable cross section*, Precision Engineering, Vol. 38(4), 915-920, 2014.
- [5] Choi, K.,B., Kim, D.,H., *Monolithic parallel linear compliant mechanism for two axes ultraprecision linear motion*, Review of Scientific Instruments, Vol. 77(6), 065106, 2006.
- [6] Choi K.,B., *Dynamics of a compliant mechanism based on flexure hinges*, Proc. ImechE Vol. 219(2) Part C: Journal of Mechanical Engineering Science, 225-235, 2005.
- [7] Howell, L.L., *Compliant Mechanisms*, John Wiley & Sons, New York, 2001.
- [8] Handley, D.,C., Lu, T.,F., Yong, Y.,K., Zhang, W.,J., *A simple and efficient dynamic modelling method for compliant micropositioning mechanisms using flexure hinges*, Proceedings of SPIE - The International Society for Optical Engineering, Vol. 5276, 67-76, 2004.
- [9] Li Y., Xu Q., *Modeling and performance evaluation of a flexure-based XY parallel micromanipulator*, Mechanism and Machine Theory, Vol. 44(12), 2127-2152, 2009.
- [10] Dirksen, F., Lammering, R., *On mechanical properties of planar flexure hinges of compliant mechanisms*, Mechanical Sciences, Vol. 2(1), 109-117, 2011.

- [11] Yuanqiang L., Wangyu L., Lei W., *Analysis of the displacement of lumped compliant parallel-guiding mechanism considering parasitic rotation and deflection on the guiding plate and rigid beams*, Mechanism and Machine Theory, Vol. 91, 50-68, 2015.
- [12] Šalinić, S., Nikolić, A., *A new pseudo-rigid-body model approach for modeling the quasi-static response of planar flexure-hinge mechanisms*, (submitted to a journal), 2017.
- [13] Lobontiu, N., *Compliance-based matrix method for modeling the quasi-static response of planar serial flexure-hinge mechanisms*, Precision Engineering, Vol. 38(3), 639-650, 2014.
- [14] Paros, J.,M., Weisbord, L., *How to design flexure hinges*, Machine Design, Vol. 37, 151-156, 1965.
- [15] Koseki, Y., Tanikawa, T., Koyachi, N., Arai, T., *Kinematic analysis of a translational 3-DOF micro-parallel mechanism using the matrix method*, Advanced Robotics, Vol. 16(3), 251-264, 2002.
- [16] Pavlović, N.,D., Pavlović, N.,T., *Compliant Mechanisms*, Faculty of Mechanical Engineering, University of Niš, Niš, 2013.
- [17] Lurie, A.,I., *Analytical Mechanics*, Springer-Verlag, New York, 2002.
- [18] Meirovitch, L., *Fundamentals of Vibrations*, McGraw-Hill, New York, 2001.
- [19] Yong, Y.,K., Lu, T.,F., *The effect of the accuracies of flexure hinge equations on the output compliances of planar micro-motion stages*, Mechanism and Machine Theory, Vol. 43(3), 347-363, 2008.
- [20] Schotborgh, W.,O., Kokkeler, F.,G.,M., Tragter, H., Van Houten, F.,J.,A.,M., *Dimensionless design graphs for flexure elements and a comparison between three flexure elements*, Precision Engineering, Vol. 29(1), 41-47, 2005.